Short time interval for condensation of high-temperature silicates in the solar accretion disk

Tu-Han Luu[a,b,1], Edward D. Young[c], Matthieu Gounelle[d,e], and Marc Chaussidon[b]

[a]Centre de Recherches Pétrographiques et Géochimiques (CRPG) - Institut National des Sciences de l'Univers CNRS - Université de Lorraine - UMR 7358, 54501 Vandoeuvre-lès-Nancy Cedex, France; [b]Institut de Physique du Globe de Paris (IPGP), CNRS UMR 7154, Sorbonne Paris Cité, 75238 Paris Cedex 05, France; [c]Department of Earth, Planetary, and Space Sciences, University of California, Los Angeles, CA 90095-1567; [d]Institut de Minéralogie et de Physique des Milieux Condensés, Muséum National d'Histoire Naturelle, Sorbonne Universités, CNRS, Université Pierre et Marie Curie & L'Institut de Recherche pour le Développement, 75005 Paris, France; and [e]Institut Universitaire de France, 75005 Paris, France

Edited by Mark H. Thiemens, University of California, San Diego, La Jolla, CA, and approved December 12, 2014 (received for review July 23, 2014)

Chondritic meteorites are made of primitive components that record the first steps of formation of solids in our Solar System. Chondrules are the major component of chondrites, yet little is known about their formation mechanisms and history within the solar protoplanetary disk (SPD). We use the reconstructed concentrations of short-lived ^{26}Al in chondrules to constrain the timing of formation of their precursors in the SPD. High-precision bulk magnesium isotopic measurements of 14 chondrules from the Allende chondrite define a ^{26}Al isochron with $^{26}Al/^{27}Al$ = 1.2(±0.2) × 10^{-5} for this subset of Allende chondrules. This can be considered to be the minimum bulk chondrule ^{26}Al isochron because all chondrules analyzed so far with high precision (∼50 chondrules from CV and ordinary chondrites) have an inferred minimum bulk initial ($^{26}Al/^{27}Al$) ≥ 1.2 × 10^{-5}. In addition, mineral ^{26}Al isochrons determined on the same chondrules show that their formation (i.e., fusion of their precursors by energetic events) took place from 0 Myr to ∼2 Myr after the formation of their precursors, thus showing in some cases a clear decoupling in time between the two events. The finding of a minimum bulk chondrule ^{26}Al isochron is used to constrain the astrophysical settings for chondrule formation. Either the temperature of the condensation zone dropped below the condensation temperature of chondrule precursors at ∼1.5 My after the start of the Solar System or the transport of precursors from the condensation zone to potential storage sites stopped after 1.5 My, possibly due to a drop in the disk accretion rate.

Mg isotope analyses | MC-SIMS | HR-MC-ICPMS | chondrule history | short-lived ^{26}Al

Primitive meteorites (i.e., chondrites) are rocks that escaped melting and differentiation on their parent bodies. As a result, their components preserved a record of the mineralogy, chemistry, and isotopic compositions of the solids formed in the solar protoplanetary disk (SPD) before planetesimal formation. Viscous heating in the inner regions of the SPD (1) brought presolar dust and gas to temperatures higher than the sublimation point of most minerals, producing a gas that upon cooling produced the first Solar System solids by condensation. The relative uniformity of isotope ratios among many early Solar System materials (2) is testament to this phase of homogenization. The calcium–aluminum-rich inclusions (CAIs) that are found in primitive meteorites are considered to be formed from refractory precursors condensed at temperatures in the range from ∼1,400 K to ∼1,800 K (3). Chondrules are millimeter-size once-molten silicate spherules that comprise most of the mass (70–80%) of chondrites. They have compositions indicating that their formation took place from solid precursors condensed below 1,500 K (4, 5). The exact timing (duration, chronology) of (*i*) the condensation processes that produced the precursors of CAIs and of chondrules, and (*ii*) the processes that resulted in the formation of CAIs and chondrules, is still poorly known, although it is key to a better understanding of the complex origin and evolution of solids in the solar accretion disk.

The radionuclide ^{26}Al decays to ^{26}Mg with a half-life of 0.72 Myr and correlations between excess ^{26}Mg and Al/Mg in meteoritical materials are tell-tale signatures of ^{26}Al decay. These correlations define ^{26}Al–^{26}Mg isochrons. Major recent advances have been obtained from the development of high-precision measurements of the Mg isotopic compositions of CAIs and chondrules (6–10), increasing the resolution of ^{26}Al–^{26}Mg chronology. The existence of a bulk CV CAI ^{26}Al–^{26}Mg isochron, defined by a very tightly constrained slope and intercept in excess ^{26}Mg vs. Al/Mg space, shows that CV CAIs and their precursors formed in a very short time interval, within less than ∼40,000 years (7, 8) or even less than ∼4,000 years (11). We note, however, that some CAIs and ultrarefractory grains show evidence of heterogeneity in both $\delta^{26}Mg^*$ (initial excess $^{26}Mg/^{24}Mg$ in per mil) and initial $^{26}Al/^{27}Al$ (12–15). The existence of a well-defined bulk CAI isochron demonstrates that agglomeration, melting, and crystallization to form CAIs from their precursor materials might be considered as a single astrophysical event. This CAI formation event, or short period, is generally taken as the "time zero" of the Solar System (referred to as CAIs' age). It can be dated using the absolute U-corrected Pb-Pb chronometer to 4567.30(±0.16) My (16), with older ages up to 4,568.2 being also proposed (17). ^{26}Al studies of CAIs show that some of them were reheated and remelted later in the disk, mostly within the first few hundred thousand years and up to ∼1.8 My later in one case, but the formation of their precursors by recondensation of sublimated presolar solids can be demonstrated to have occurred at time 0, within a few tens of thousands of years (18).

The majority of the solids in the accretion disk formed at lower temperatures than did CAIs, suggesting that they also formed later or at the same time but at different heliocentric distances. The chronology of formation of the ferromagnesian material comprising the major proportion of primitive meteoritical

Significance

Combining bulk and in situ Mg isotope measurements allows dating the formation of chondrule precursors relative to that of chondrules themselves. This has never been achieved before and has profound implications for the origin of chondrules, the origin of their precursors, and the evolution of the solar protoplanetary disk. There is a minimum bulk chondrule isochron, analogous in some ways to the bulk calcium–aluminum-rich inclusion isochron, which dates either the cessation of condensation of chondrule precursors or the cessation of their transport to the regions where chondrules formed.

Author contributions: T.-H.L., E.D.Y., M.G., and M.C. analyzed data and wrote the paper.

The authors declare no conflict of interest.

This article is a PNAS Direct Submission.

[1]To whom correspondence should be addressed. Email: luu@crpg.cnrs-nancy.fr.

This article contains supporting information online at www.pnas.org/lookup/suppl/doi:10.1073/pnas.1414025112/-/DCSupplemental.

materials (e.g., chondrules) has proven elusive. Most chondrule age dating comes from evidence for the concentrations of short-lived ^{26}Al and to a lesser extent ^{53}Mn in the objects. A time gap of a few million years between CAIs and chondrules (with peaks of chondrule formation between ∼1.5 My and 3 My) is a general conclusion of ^{26}Al studies based on mineral isochrons (e.g., refs. 9, 19, and 20). However, this conclusion relies on the assumption of homogeneity of the ^{26}Al distribution at time 0 in the inner region of the disk [see discussions on ^{26}Al distribution in Villeneuve et al. (9), Larsen et al. (11), and Mishra and Chaussidon (21)]. In addition, mineral ^{26}Al isochrons in chondrules date the last melting event, thus giving no clue on the age of formation of chondrule precursors. In one case, the age of chondrule precursors could be determined using ^{26}Al systematics by calculating a model age from the Mg isotopic composition. This approach gives a precursor age of 0.87(±0.20) My after CAIs for a chondrule which was last melted ∼4 My post-CAI (9), bringing the formation of chondrule precursors closer to that of CAIs. Uranium-isotope-corrected Pb–Pb dating of chondrules are very scarce but recent data do show a ∼3-Myr age range, with several chondrules as old as CAIs, at 4,567.32 ± 0.42 My and 4,566.67 ± 0.43 My (16), as also suggested by ^{53}Mn data (22, 23). The temporal relationships between chondrule precursors and the chondrule formation events are therefore not well understood, especially because of a lack of comprehensive measurements in the same set of objects.

Here we report the Mg isotope study of 14 Mg-rich (type I) and Al-rich chondrules from the Allende carbonaceous chondrite (CV3). Our approach is, for the first time to our knowledge, to look both for mineral ^{26}Al isochrons and bulk ^{26}Al isochrons in the same chondrules. This is done by combining the use of multicollector secondary ion mass spectrometry (MC-SIMS) on eight chondrules for in situ analyses (at CRPG-CNRS Nancy, France) and high-resolution multicollector inductively coupled plasma source mass spectrometry (HR-MC-ICPMS) on 14 chondrules (the same as the ones measured by MC-SIMS, plus six others) for bulk analyses (at IPG Paris and CRPG-CNRS Nancy, France and at University of California, Los Angeles). Note that for Ch#B, three fragments of this chondrule (named Ch#B1, Ch#B2, and Ch#B3) were measured for their bulk Mg isotopic composition. This approach allows us to determine the age of chondrule precursors and the age of their last melting event using multiple lines of evidence. Results constrain the timing of condensation, transport, melting, and accretion of solids in the accretion disk.

Results

The chondrules studied from the Allende CV3 chondrite (see *SI Appendix, SI Materials and Methods*, *SI 2A*, and *SI 2B*) have bulk ^{27}Al/^{24}Mg ratios varying from 0.051 to 1.815 (Table 1), i.e., in the typical range for ferromagnesian to Al-rich chondrules [the latter having >10 wt% bulk Al_2O_3 (24)]. All bulk measurements (Table 1 and Fig. 1) together define a ^{26}Al isochron with a slope corresponding to an initial (^{26}Al/^{27}Al), $(^{26}Al/^{27}Al)_{bulk\ initial}$, of $1.23(\pm0.21) \times 10^{-5}$ and an intercept, $(\delta^{26}Mg^*)_{bulk\ initial}$, of −0.009(±0.012)‰ [mean square weighted deviation (MSWD) = 0.62], clearly distinct from those of the bulk CAI isochron [with $(^{26}Al/^{27}Al)_0 = 5.25(\pm0.12) \times 10^{-5}$ and $(\delta^{26}Mg^*)_0 = -0.034(\pm0.032)$‰, where the zero subscript refers to the CAI initial values, as calculated from data by Jacobsen et al. (7) and Larsen et al. (11)]. Assuming ^{26}Al homogeneity in the inner Solar System, this chondrule whole-rock slope of $1.23(\pm0.21) \times 10^{-5}$ would correspond to an age of 1.53(±0.18) My after CAI formation. One chondrule (Ch#1) has a bulk radiogenic ^{26}Mg excesses, which could also be consistent with the bulk CAI isochron. Excluding Ch#1 does not change significantly the bulk chondrule isochron [$(^{26}Al/^{27}Al)_{bulk\ initial} = 1.25(\pm0.21) \times 10^{-5}$ and $(\delta^{26}Mg^*)_{bulk\ initial} = -0.012(\pm0.013)$‰, MSWD = 0.18]. Although Mg evaporative loss does not always result in Mg isotopic fractionation (25, 26), there is no apparent correlation between the bulk ^{27}Al/^{24}Mg ratios and δ^{25}Mg values that would be indicative of such a process during chondrule melting. This suggests that chondrule precursors were never molten in a free vacuum and points to a high mass density of chondrules and their precursors (26). Investigations in more details of three Al-rich chondrules, which are key for the bulk chondrule isochron, showed no detectable effect of metamorphism and/or alteration on the Mg isotopic systematics (see *SI Appendix, SI 2B*).

At the mineral scale within a single chondrule, the ^{27}Al/^{24}Mg ratios are much more variable: A range of a factor of 10 is

Table 1. Chemistry, Mg isotope bulk data, and ^{26}Al mineral isochrons

		$(^{27}Al/^{24}Mg)_{bulk}$		$(\delta^{25}Mg)_{bulk}$ (‰)		$(\delta^{26}Mg^*)_{bulk}$ (‰)			$(^{26}Al/^{27}Al)_i$		$(\delta^{26}Mg^*)_i$ (‰)		
Chondrule	Type	Value	2σ	Value	2σ	Value	2σ	n	Value	2σ	Value	2σ	n
Ch#1	PP	0.347	0.035	−0.151	0.044	0.075	0.047	8	2.59×10^{-5}	1.53×10^{-5}	0.063	0.029	10
Ch#2	IO	0.135	0.008	−0.132	0.047	0.013	0.042	7					
Ch#5	PO	0.128	0.006	−0.111	0.052	0.008	0.051	7	3.48×10^{-6}	5.71×10^{-6}	0.018	0.026	9
Ch#6	PO	0.118	0.014	−0.143	0.042	0.003	0.043	7					
Ch#10	PO	0.099	0.002	−0.094	0.050	−0.007	0.046	7	8.78×10^{-6}	6.27×10^{-6}	0.008	0.019	10
Ch#12	PO	0.062	0.005	−0.174	0.043	−0.009	0.046	8	2.29×10^{-5}	1.09×10^{-5}	−0.015	0.027	15
Ch#15	PO	0.078	0.003	−0.156	0.051	−0.008	0.042	7					
Ch#18	BO	0.121	0.001	−0.387	0.046	−0.006	0.046	7					
Ch#20		0.051	0.002	−0.168	0.046	−0.002	0.047	7					
Ch#21	BO	0.076	0.005	−0.106	0.044	−0.005	0.044	7	1.17×10^{-5}	3.76×10^{-6}	−0.047	0.024	15
Ch#A	PO	0.086	0.060			0.002	0.027		2.38×10^{-5}	6.97×10^{-6}	−0.006	0.026	26
Ch#B1	Al-rich	1.375	0.072			0.127	0.014						
Ch#B2		1.710	0.068			0.152	0.034						
Ch#B3		2.359	0.057			0.184	0.020						
Ch#B		1.815	0.066			0.154	0.023		1.06×10^{-5}	1.39×10^{-6}	0.030	0.015	35
Ch#C	Al-rich	0.663	0.060			0.038	0.028		1.56×10^{-5}	1.95×10^{-6}	0.029	0.018	36
Ch#D	Al-rich	0.527	0.060			0.024	0.031						

BO, barred olivine; IO, isolated olivine; PO, olivine-rich porphyritic; PP, pyroxene-rich porphyritic. Ch#B1, Ch#B2, and Ch#B3 represent three fragments of the same chondrule. The average of these three fragments (named Ch#B) is used as the bulk value and is represented on Fig. 1 (the three fragments are represented by orange diamonds while the average is in blue). Data for chondrules Ch#A, Ch#B, Ch#C, and Ch#D were previously reported in Ingalls et al. (46), where they were named Allende CH1, CH2, CH3, and CH4, respectively.

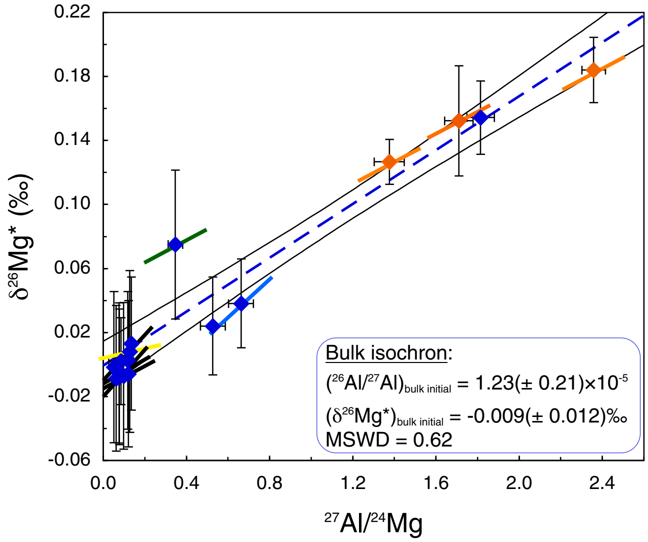

Fig. 1. Comparison between bulk and mineral ^{26}Al isochrons for the 14 Allende chondrules from this study. The best-fit line yields a bulk isochron (blue dashed line defined by the blue diamonds) with a $(^{26}Al/^{27}Al)_{bulk\ initial}$ slope of 1.23(±0.21) × 10^{-5} and an intercept $(\delta^{26}Mg^*)_{bulk\ initial}$ of −0.009(±0.012)‰. The mineral ^{26}Al isochrons are represented for each object by the colored segments passing through the bulk compositions. By definition, the slope of the mineral isochron cannot be higher than that of the bulk isochron since the formation of the chondrule itself cannot predate the formation of its precursors. This is verified by nearly all chondrules except a few that might have in fact a bulk $^{26}Al/^{27}Al$ ratio higher than that of the bulk chondrule isochron (see text).

present in Ch#1 and up to a factor of ∼335 in Ch#B. This range in composition allowed for determination of mineral ^{26}Al isochrons for each chondrule, although not all of the isochrons are well defined. These ^{26}Al mineral isochrons (see individual diagrams in *SI Appendix, SI 2C*) show slopes corresponding to $(^{26}Al/^{27}Al)_i$ from 3.48(±5.71) × 10^{-6} to 2.59(±1.53) × 10^{-5}, and $(\delta^{26}Mg^*)_i$ intercepts from −0.047(±0.024)‰ to 0.063(±0.029)‰ (Table 1). This is consistent with previous mineral isochrons [3 × 10^{-6} < $(^{26}Al/^{27}Al)_i$ < 1 × 10^{-5} for chondrules in LL3.0 chondrites (9, 20, 27–29), CO3.0 chondrites (20, 30, 31), and Acfer 094 (Ungrouped C 3.0; 20, 32, 33)]. The $(^{26}Al/^{27}Al)_i$ ratios are higher than, equal to, or lower than $(^{26}Al/^{27}Al)_{bulk\ initial}$ depending on the chondrules (Fig. 1). There is no clear relationship between the $(^{26}Al/^{27}Al)_i$ ratios and $(\delta^{26}Mg^*)_i$ values, or between the $(^{26}Al/^{27}Al)_i$ ratios and the bulk $^{27}Al/^{24}Mg$ ratios. Assuming ^{26}Al homogeneity in the inner Solar System, the $(^{26}Al/^{27}Al)_i$ ratios of the chondrule mineral isochrons correspond to an average age of 1.2 My after CAI formation [total range from 0.73(+0.93/−0.48) to 1.86(+1.30/−0.56) My after CAIs]. Ch#5 is the only chondrule which has a significantly lower $(^{26}Al/^{27}Al)_i$ corresponding to a younger age of 2.81(±1.00) My after CAIs.

Constraints from the Bulk ^{26}Al Isochron on the Age of Chondrule Precursors

The simplest interpretation of a bulk composition of a chondrule is to consider that it reflects the average composition of its solid precursors. Assuming that ^{26}Al and Mg isotopes were homogenized to ∼±10% at time 0 in the regions of the SPD where the precursors of CAIs and chondrules formed (9, 21), the present bulk chondrule ^{26}Al isochron with $(^{26}Al/^{27}Al)_{bulk\ initial}$ = 1.23(±0.21) × 10^{-5} would measure the average age of the precursors of the 14 Allende chondrules studied relative to CAIs under the assumption that chondrules and CAIs are averages of the same materials sampled at different times. In this case, chondrule precursors formed 1.53(±0.18) My after CAIs. Using the same reasoning as that used to constrain CAI precursors formation times from the bulk CAI ^{26}Al isochron (8, 11), the scatter of data around the bulk chondrule isochron would indicate that the precursors of the present chondrules formed over a short period (< 180 kyr).

However, this conclusion does not seem to be valid for chondrules in general when considering all existing high-precision Mg isotopic data for bulk chondrules [Galy et al. (34) and Bizzarro et al. (35) for the Allende CV3 carbonaceous chondrite, and bulk compositions recalculated from data by Villeneuve et al. (9) for the Semarkona LL3 ordinary chondrite]. A significant number of chondrules plot on the bulk CAI isochron and five chondrules plot in between the bulk CAI isochron and the bulk chondrule isochron from this study (Fig. 2). In addition, because "normal" ferromagnesian chondrules have low $^{27}Al/^{24}Mg$ ratios (<0.2), they cannot develop high enough $^{26}Mg^*$ excesses (relative to the analytical uncertainties) to distinguish between the two isochrons (Fig. 2). Seven chondrules with high $^{27}Al/^{24}Mg$ ratios [three from this study, one from Galy et al. (34), two from Bizzarro et al. (35), and one from Villeneuve et al. (9)], plot unambiguously on the bulk chondrule isochron defined herein (Fig. 2). The regression line calculated from these seven chondrules corresponds to $(^{26}Al/^{27}Al)_{bulk\ initial}$ = 1.30(±0.20) × 10^{-5} and $(\delta^{26}Mg^*)_{bulk\ initial}$ = −0.013(±0.005)‰, with an MSWD = 1.1, and is identical within errors to that calculated from all of the chondrules from this study, thus confirming the robustness of this isochron.

It is tempting to ascribe the distribution of chondrules between the bulk CAI isochron and the present bulk chondrule isochron (Fig. 2) to the formation of chondrule precursors starting contemporaneously with the formation of CAI precursors and ending ∼1.5 Myr later. However, we note that the bulk Mg isotopic data do not exclude the possibility that all chondrule precursors formed at the same time as CAI precursors (or very close to CAI precursors). This is because Mg isotopic compositions of chondrules could have been reset during chondrule forming events by high-temperature Mg isotopic exchange with the nebular gas, producing an ^{26}Al isochron with a $^{26}Al/^{27}Al$ slope and initial $\delta^{26}Mg^*$ intercept corresponding to the isotopic composition of the gas at the time. When $^{26}Al/^{27}Al$ decreased to 1.3 × 10^{-5} (i.e., 1.5 My after CAI) in a nebular gas with initial Al and Mg isotopic compositions identical to that defined by the bulk CAI isochron, the Mg isotopic composition calculated for the gas

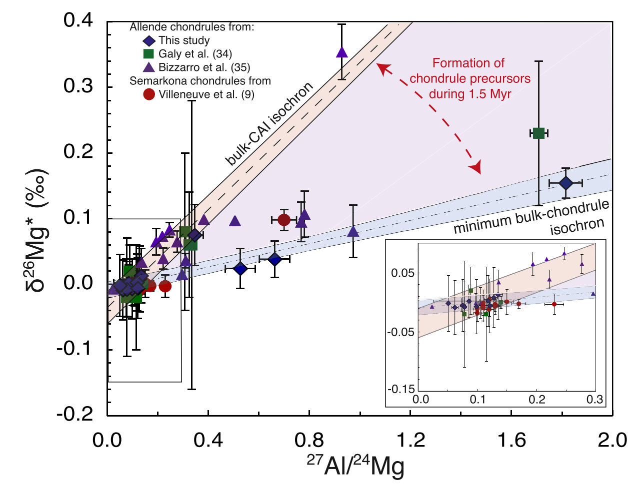

Fig. 2. ^{26}Al–^{26}Mg isochron diagram for bulk chondrules, with all available data. All chondrules plot between the bulk CAI isochron (or on it) and the minimum bulk chondrule isochron determined in this study (or on it). The minimum bulk chondrule isochron might date the end of the formation of chondrule precursors in the disk, 1.5(±0.2) My after time 0. The 2-sigma error bars are shown when larger than the data points.

gives a new radiogenic Mg isotopic composition of $\delta^{26}Mg^* = -0.007‰$. This would be consistent with the present bulk chondrule isochron. However, had this resetting happened for chondrules, it should have occurred for CAIs, too. The absence of CAIs plotting on the chondrule isochron argues in favor of a genuine difference between chondrules and CAIs. Thus, we propose that the present bulk chondrule ^{26}Al isochron (defined from a subset of Allende chondrules) can be considered as the minimum bulk chondrule ^{26}Al isochron. If this interpretation is correct, this would imply that there is in chondrites no chondrule existing with precursors formed in the SPD by nebular processes later than ~1.5 My after the start of the Solar System [chondrules formed by impact between planetesimals can be made later (36)].

Time Difference Between the Formation of Chondrules and That of Their Precursors as Indicated by the Mineral and Bulk ^{26}Al Isochrons

Further insights into the timing of formation of the Allende chondrules from this study and of their precursors can be obtained by comparing the mineral ^{26}Al isochron of each chondrule to the bulk chondrule ^{26}Al isochron. This can also be done for chondrules from Villeneuve et al. (9) for which the bulk $\delta^{26}Mg^*$ values can be recalculated from the mineral isochrons and the bulk $^{27}Al/^{24}Mg$ ratios. The bulk chondrule ^{26}Al isochron dates the time when the bulk $^{27}Al/^{24}Mg$ ratio of the precursors was established (e.g., during their formation by condensation from the gas), while the mineral isochron dates the time when the $^{27}Al/^{24}Mg$ ratios were fractionated between the different components of a chondrule by crystallization during the last chondrule melting event. Because final crystallization must postdate establishment of the precursor chemistry, it is expected that all chondrules should exhibit mineral isochrons with slopes $[(^{26}Al/^{27}Al)_i]$ lower than, or equal to, the slope of the bulk chondrule isochron $[(^{26}Al/^{27}Al)_{bulk\ initial}]$. For internal consistency, we also expect that the initial $\delta^{26}Mg^*$ ($\delta^{26}Mg^*_i$, intercepts) of the mineral isochrons should be greater than, or equal to, that of the bulk isochron and that the differences in initial $\delta^{26}Mg^*$ should be consistent with the differences in slopes (i.e., initial $^{26}Al/^{27}Al$) between the mineral and bulk isochrons.

This check on internal consistency is verified for Ch#5, Ch#10, Ch#21, Ch#B, Ch#C, and all chondrules from Villeneuve et al. (9). Ch#10, Ch#21, Ch#B, and Ch#C have $(^{26}Al/^{27}Al)_i$ ratios identical within errors with the $(^{26}Al/^{27}Al)_{bulk\ initial}$ ratio (Fig. 1), in agreement either with formation of their precursors contemporaneously with chondrule melting or Mg isotopic reequilibration with the nebular gas during chondrule melting. As discussed in *Constraints from the Bulk ^{26}Al Isochron*, the present data do not provide the basis for favoring one hypothesis or the other definitively. Ch#5 and all chondrules from Villeneuve et al. (9) have $(^{26}Al/^{27}Al)_i$ ratios that are significantly lower [e.g., $4.2(\pm5.3) \times 10^{-6}$] than the $(^{26}Al/^{27}Al)_{bulk\ initial}$ ratio of $1.3(\pm0.2) \times 10^{-5}$. This implies that the last melting event that affected these chondrules took place later than the formation of their precursors. For example, for Ch#5, the youngest possible age for the formation of chondrule precursors constrained by the minimum bulk chondrule isochron being ~1.5 My after CAIs is 2.8(±1.0) My after CAIs; chondrules were being reset for at least ~1 Myr, if not longer.

Two chondrules exhibit $(^{26}Al/^{27}Al)_i$ ratios defined by their constituent minerals higher than the $(^{26}Al/^{27}Al)_{bulk\ initial}$ ratio defined in this study: This is the case for Ch#A $[(^{26}Al/^{27}Al)_i = 2.0(\pm0.4) \times 10^{-5}]$ and marginally for Ch#12 $[(^{26}Al/^{27}Al)_i = 2.0(\pm0.9) \times 10^{-5}]$. Because these two chondrules have low $^{27}Al/^{24}Mg$ bulk ratios (0.062 and 0.086 for Ch#12 and Ch#A, respectively), their bulk $\delta^{26}Mg^*$ values plot between the bulk chondrule isochron of this study and the bulk CAI isochron (Fig. 2). The mineral isochrons imply that the precursors of Ch#A (and possibly of Ch#12) formed when $^{26}Al/^{27}Al$ was $\geq 2.0 \times 10^{-5}$ in the SPD and perhaps when it was as high as 5.2×10^{-5}.

^{26}Al Model Ages of Chondrule Precursors

When chondrules have $^{27}Al/^{24}Mg$ ratios significantly higher than chondritic (the case of Al-rich chondrules), a ^{26}Al model age of their precursors can be calculated relative to the Solar System growth curve of $\delta^{26}Mg^*$, as explained in Villeneuve et al. (9). These model ages record the time of separation of the material from the bulk, or average, solar reservoir (in this case, the enrichment in Al). In a diagram showing $(\delta^{26}Mg^*)_i$ versus $(^{26}Al/^{27}Al)_i$ (i.e., time), any excess in ^{26}Mg relative to the growth curve of the Solar System (anchored by the composition defined by the bulk CAI isochron and calculated for a Solar System $^{27}Al/^{24}Mg$ ratio of 0.101) can be explained by ^{26}Al decay in a closed system comprising the chondrule's Al-rich precursors. This evolution is defined by the following:

$$(\delta^{26}Mg^*)_i = (\delta^{26}Mg^*)_0 + \frac{1{,}000}{0.13932} \times \left[\left(\left(\frac{^{26}Al}{^{27}Al}\right)_0 - \left(\frac{^{26}Al}{^{27}Al}\right)_{precursors}\right) \times \left(\frac{^{27}Al}{^{24}Mg}\right)_{Solar} + \left(\left(\frac{^{26}Al}{^{27}Al}\right)_{precursors} - \left(\frac{^{26}Al}{^{27}Al}\right)_i\right) \times \left(\frac{^{27}Al}{^{24}Mg}\right)_{precursors}\right] \quad [1]$$

where $(^{26}Al/^{27}Al)_{precursors}$ is the $^{26}Al/^{27}Al$ ratio at the time of formation of Al-rich precursors, $(^{27}Al/^{24}Mg)_{precursors}$ is the $^{27}Al/^{24}Mg$ of the precursors assumed to be the bulk ratio of the chondrule, and 0.13932 is the reference $^{26}Mg/^{24}Mg$ ratio. In this two-stage model, it is assumed that between $(^{26}Al/^{27}Al)_0$ and $(^{26}Al/^{27}Al)_{precursors}$ (i.e., between the solar initial $^{26}Al/^{27}Al$ defined by CAIs and the initial $^{26}Al/^{27}Al$ of the chondrule precursors), the evolution of Mg isotopes takes place in the SPD gas with the solar $^{27}Al/^{24}Mg$ ratio, and that at the time given by the intersection between the chondrules growth curve and the Solar System growth curve, chondrule precursors formed with $(^{27}Al/^{24}Mg)_{precursors}$. Precursors model ages can be calculated for one chondrule from Villeneuve et al. (9) and three chondrules from the present study (Fig. 3). This gives 0 ± 0.12 My for Ch#1, 0.87 ± 0.20 My for Sem-ch4 from ref. 9, 1.12 ± 0.52 My for Ch#C, and 1.51 ± 0.17 My for Ch#B (Fig. 3; see *SI Appendix, SI Materials and Methods* for details of error propagation). These ages represent the formation time of the material from which the chondrules formed. Ch#B and Ch#C plot on the bulk chondrule isochron, indicating that their precursors formed at 1.5 ± 0.2 My. Conversely, Ch#1 and Sem-ch4 are evidently composed of precursors formed much earlier, dating all of the way back to CAI formation in the case of Ch#1 (see, in *SI Appendix, Possible Fraction of CAI Material in Al-Rich Chondrules*, an alternative explanation of Ch#1 composition).

Arguments For and Against ^{26}Al Homogeneity in the CAIs- and Chondrules-Forming Region of the Disk

All of the present Mg isotopic data can be understood in the context of homogeneous, or nearly homogeneous, $^{26}Al/^{27}Al$ and Mg isotope ratios in the regions of the accretion disk where CAIs, chondrules, and their precursors formed. In this case, variable initial $^{26}Al/^{27}Al$ and $\delta^{26}Mg^*$ values have a chronological significance. Similar observations were made previously for chondrules (9) and CAIs (21). However, other observations exist that are used to suggest significant heterogeneity in these isotope ratios from ultra-high-precision (a few parts per million level) Mg isotopic composition of CAIs and AOAs (11) or from apparent age discrepancies between the Pb–Pb and ^{26}Al chondrule age dates (16). We explore in the following if the chondrule Mg isotopic data presented here can be understood in the context of $^{26}Al/^{27}Al$ heterogeneity and what the consequences would be

EARTH, ATMOSPHERIC, AND PLANETARY SCIENCES

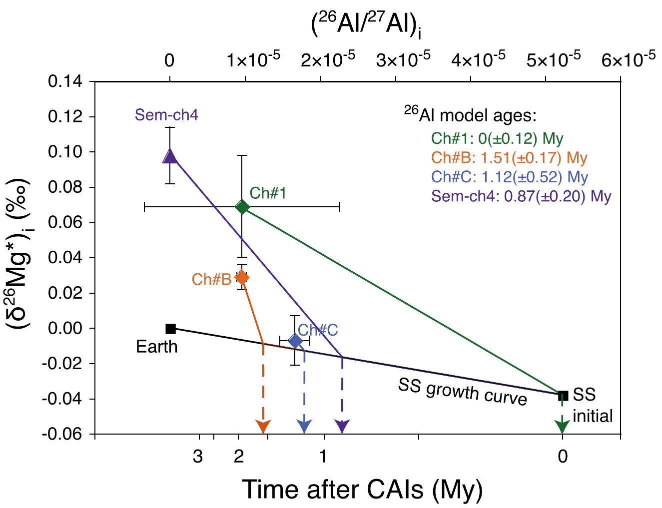

Fig. 3. ^{26}Al model ages of the precursors of 4 FeO-poor type I chondrules [Ch#1, Ch#B, and Ch#C from this study, Sem-ch4 from Villeneuve et al. (9)] calculated from the intersection between the Solar System (SS) ^{26}Mg growth curve (black line) and the chondrules ^{26}Mg growth curves (colored lines). The SS growth curve is anchored by the (^{26}Al/^{27}Al)$_0$ and (δ^{26}Mg*)$_0$ of bulk CAIs, and is calculated for a solar ^{27}Al/^{24}Mg ratio of 0.101 (47). The chondrule growth curves are anchored by the (^{26}Al/^{27}Al)$_i$ and (δ^{26}Mg*)$_i$ of bulk chondrules, and calculated using the bulk ^{27}Al/^{24}Mg ratios of each chondrule assuming that this is bulk composition of their precursors and that they evolved in closed system between their accretion and chondrule melting (see *^{26}Al Model Ages of Chondrule Precursors* for details). This gives precursor ^{26}Al model ages of 0(±0.12) My for Ch#1, 1.51(±0.17) My for Ch#B, 1.12(±0.52) My for Ch#C, and 0.87(±0.20) My for Sem-ch4.

for our understanding of the formation of chondrules and their precursors.

Because all chondrules show ^{26}Al mineral isochrons having similar initial δ^{26}Mg* values, the only scenario for heterogeneous distribution that would be consistent with the chondrule data is one in which most of the heterogeneity is due to variations in the ^{26}Al/^{27}Al ratio of the nebular gas and not to large variations in its δ^{26}Mg* value. To explain the minimum bulk chondrule ^{26}Al isochron by heterogeneity in ^{26}Al/^{27}Al, two gaseous reservoirs should have coexisted at time 0 (given by the bulk CAI isochron and corresponding to an absolute age of ~4,568 My; see the Introduction), one with ^{26}Al/^{27}Al = 5.2 × 10^{-5} and one with ^{26}Al/^{27}Al = 1.2 × 10^{-5}, both having similar δ^{26}Mg* values in the range from −0.034‰ to ~−0.006‰ (see *Constraints from the Bulk ^{26}Al Isochron*), and possibly similar ^{27}Al/^{24}Mg ratios. This conclusion results from the fact that it is highly unlikely that the minimum bulk chondrule ^{26}Al isochron is a mixing line between two types of components having different Mg isotopic compositions (one Mg-rich with ^{27}Al/^{24}Mg ≈ 0 and δ^{26}Mg* = −0.006‰ and the other Mg-poor with ^{27}Al/^{24}Mg ≈ 2.5 and δ^{26}Mg* ≈ +0.2‰) because the mineral isochrons demonstrate that live ^{26}Al was present in several of these chondrules at a level of (^{26}Al/^{27}Al)$_i$ ≈ 1.2 × 10^{-5}. The initial ^{26}Al/^{27}Al ratios in these objects are not readily explained as spurious products of mixing unless an extraordinary coincidence is invoked.

While unlikely on the basis of the data, the scenario of heterogeneous isotopic distribution in the disk cannot be ruled out unequivocally. However, significant heterogeneity sufficient to invalidate chronological interpretations seems unlikely for two additional reasons. First, it is difficult to understand why precursors of chondrules would be formed from the two contemporaneous gas reservoirs while precursors of CAIs formed only from the one reservoir with ^{26}Al/^{27}Al ≈ 5.25 × 10^{-5}. Second, in the scenario of isotopic homogeneity, the variations in initial ^{26}Al/^{27}Al ratios and variations in initial δ^{26}Mg* values observed in chondrules are both well explained by decay of ^{26}Al from a reservoir homogenized at time 0 (with a precision of ~10% for ^{26}Al/^{27}Al and a few parts per million for δ^{26}Mg*). This would appear to be an extraordinary coincidence in the case of isotopic heterogeneity. This later argument was previously developed in Villeneuve et al. (9) and Mishra and Chaussidon (21).

In conclusion, heterogeneity at some level must have existed in the SPD, and perhaps early or locally it was pronounced (12–14), but on a global scale for the majority of chondrules (and all chondrules in the present study), it does not seem to be a requirement from the data. This does not explain the apparent age discrepancy observed for chondrules between ^{26}Al ages and Pb–Pb ages (16) but we note that the bulk δ^{26}Mg* of chondrules (in the hypothesis of ^{26}Al homogeneity) implies that many chondrules had their precursors formed at the same time as CAIs.

Astrophysical Implications

While chondrules do not contain precursors (i.e., high-temperature condensation from a gas of solar composition) formed later than 1.5 My after "time zero," the formation of chondrules (i.e., fusion of their precursors by energetic events) took place from 0 My to ~2 My after the formation of their precursors (as shown by the present data and also, most presumably, for many chondrules from several previous studies for which the bulk δ^{26}Mg* is not available). This observation is quite interesting in the framework of most recent models of protoplanetary disks (37). The condensation of mineral precursors of chondrules occurred within the hot zone of the SPD, bound by the sublimation and condensation fronts (~isotherms) for silicates. This region, probably maintained hot by viscous heating that is the natural consequence of accretion, extended from a few tenths of an astronomical unit (AU) (38) to 1 AU or so (39). Since chondrule formation evidently occurred a few astronomical units from the star (40), it implies that chondrule precursors were transported from the inner hot disk region to the (now) region of the present-day asteroid belt. However, a transport mechanism based on the viscous expansion of the disk (41, 42) is applicable only in the case of early (within a few 10^5 years of CAI formation) condensation of chondrule precursors.

Because, in some (rare) cases, chondrule formation appears to be delayed relative to the condensation of their precursors, it implies that the precursors can be stored for times possibly as long as ~2 Myr before the energetic chondrule-forming events. The so-called dead zone, where the disk gas is immune to cosmic ray ionization and the gas flow is laminar rather than turbulent, is a region of choice to store solids, especially since the accumulation of dust does not alter its properties (43). In a majority of cases, however, it appears that the melting to form chondrules occurred contemporaneously (within errors) with the condensation of the precursors. This implies that the source of energy that caused the formation of chondrules occurred where condensation was occurring. This in turn implies that the chondrule-forming process was in the inner part of the dead zone, perhaps related to planet formation (44).

Some of the present observations could also be understood in the framework of alternative models for chondrule formation. For example, in the case of chondrule formation by solidification of melts generated by impacts between planetesimals, the age of the precursors can be viewed as the age of the planetesimals, and the age of the chondrules as the age of the collision. The storage of the precursors at the surface of planetesimals could be an alternative to their storage in a dead zone of the SPD. However, planetesimals accreted earlier than 1.5 Myr post-CAIs are likely to have experienced rock–metal differentiation (45) as a result of heating by ^{26}Al decay (assuming an initial solar ^{26}Al/^{27}Al near 5.2 × 10^{-5}), and this does not appear to be consistent with the isotopic and chemical characteristics of ferromagnesian chondrules. On the other hand, the basaltic crusts of differentiated objects should have been characterized by high $^{27}Al/^{24}Mg$ ratios and high $\delta^{26}Mg^*$ values, making them a potential source of precursors to Al-rich chondrules.

In conclusion, although we are still far from a detailed understanding of the evolution of the solar protoplanetary disk, the present ^{26}Al chondrule data help bridge the gap between the timing of processes in the SPD recorded in meteorites and modeling of physical processes such as condensation, transport, and energetic events anticipatory to, or resulting from, planet formation.

ACKNOWLEDGMENTS. This work was supported by a grant from the European Research Council (Grant FP7/2007–2013, Grant Agreement 226846: Cosmochemical Exploration of the First Two Million Years of the Solar System) and the UnivEarthS Labex program at Sorbonne Paris Cité (ANR-10-LABX-0023 and ANR-11-IDEX-0005-02). Support also came from the NASA Cosmochemistry program (E.D.Y.). This is Centre de Recherches Pétrographiques et Géochimiques (CRPG)-CNRS Contribution 2354.

1. Hueso R, Guillot T (2005) Evolution of protoplanetary disks: Constraints from DM Tauri and GM Aurigae. *Astron Astrophys* 442:703–725.
2. Trinquier A, et al. (2009) Origin of nucleosynthetic isotope heterogeneity in the solar protoplanetary disk. *Science* 324(5925):374–376.
3. Yoneda S, Grossman L (1995) Condensation of CaO-MgO-Al_2O_3-SiO_2 liquids from cosmic gases. *Geochim Cosmochim Acta* 59:3413–3444.
4. Herzberg CT (1979) The solubility of olivine in basaltic liquids: An ionic model. *Geochim Cosmochim Acta* 43:1241–1251.
5. Hewins RH, Radomsky PM (1990) Temperature conditions for chondrule formation. *Meteoritics* 25:309–318.
6. Bizzarro M, et al. (2011) High-precision Mg-isotope measurements of terrestrial and extraterrestrial material by HR-MC-ICPMS—Implications for the relative and absolute Mg-isotope composition of the bulk silicate Earth. *J Anal At Spectrom* 26:565–577.
7. Jacobsen B, et al. (2008) ^{26}Al–^{26}Mg and ^{207}Pb–^{206}Pb systematics of Allende CAIs: Canonical solar initial $^{26}Al/^{27}Al$ ratio reinstated. *Earth Planet Sci Lett* 272:353–364.
8. Thrane K, Bizzarro M, Baker JA (2006) Extremely brief formation interval for refractory inclusions and uniform distribution of ^{26}Al in the early solar system. *Astrophys J* 646:L159–L162.
9. Villeneuve J, Chaussidon M, Libourel G (2009) Homogeneous distribution of ^{26}Al in the solar system from the Mg isotopic composition of chondrules. *Science* 325(5943):985–988.
10. Luu T-H, et al. (2013) High precision Mg isotope measurements of meteoritic samples by secondary ion mass spectrometry. *J Anal At Spectrom* 28:67–76.
11. Larsen KK, et al. (2011) Evidence for magnesium isotope heterogeneity in the solar protoplanetary disk. *Astrophys J* 735:L37.
12. Liu MC, et al. (2009) Isotopic records in CM hibonites: Implications for timescales of mixing of isotope reservoirs in the solar nebula. *Geochim Cosmochim Acta* 73:5051–5079.
13. Liu MC, Chaussidon M, Goepel C, Lee T (2012) A heterogeneous solar nebula as sampled by CM hibonite grains. *Earth Planet Sci Lett* 327:75–83.
14. Makide K, et al. (2011) Heterogeneous distribution of ^{26}Al at the birth of the Solar System. *Astrophys J* 733:L31–L35.
15. Wasserburg GJ, Wimpenny J, Yin QZ (2012) Mg isotopic heterogeneity, Al Mg isochrons, and canonical $^{26}Al/^{27}Al$ in the early Solar System. *Meteorit Planet Sci* 47:1980–1997.
16. Connelly JN, et al. (2012) The absolute chronology and thermal processing of solids in the solar protoplanetary disk. *Science* 338(6107):651–655.
17. Bouvier A, Wadhwa M (2010) The age of the Solar System redefined by the oldest Pb-Pb age of a meteoritic inclusion. *Nat Geosci* 3:637–641.
18. MacPherson GJ, Kita NT, Ushikubo T, Bullock ES, Davis AM (2012) Well-resolved variations in the formation ages for Ca−Al-rich inclusions in the early Solar System. *Earth Planet Sci Lett* 331:43–54.
19. Kita NT, et al. (2005) Constraints on the origin of chondrules and CAIs from short-lived and long-lived radionuclides. *Chondrites and the Protoplanetary Disk*, eds Krot AN, Scott ERD, Reipurth B, ASP Conference Series (Astron Soc Pacific, San Francisco), Vol 341, pp 558–587.
20. Kita NT, Ushikubo T (2012) Evolution of protoplanetary disk inferred from ^{26}Al chronology of individual chondrules. *Meteorit Planet Sci* 47:1108–1119.
21. Mishra RK, Chaussidon M (2014) Timing and extent of Mg and Al isotopic homogenization in the early inner Solar System. *Earth Planet Sci Lett* 390:318–326.
22. Yin Q-Z, et al. (2009) ^{53}Mn-^{53}Cr systematics of Allende chondrules and $\varepsilon^{54}Cr$-$\Delta^{17}O$ correlation in bulk carbonaceous chondrites. *Lunar Planet Sci Conf* 40:2006.
23. Yin Q-Z, Yamakawa A, Sanborn M, Yamashita K (2013) Allende chondrule chronology revisited: Eroding age gap between CAIs and chondrules. *Mineral Mag* 77(5):2559.
24. Bischoff A, Keil K (1984) Al-rich objects in ordinary chondrites: Related origin of carbonaceous and ordinary chondrites and their constituents. *Geochim Cosmochim Acta* 48:693–709.
25. Richter FM (2004) Timescales determining the degree of kinetic isotope fractionation by evaporation and condensation. *Geochim Cosmochim Acta* 68:4971–4992.
26. Young ED, Galy A (2004) The isotope geochemistry and cosmochemistry of magnesium. *Rev Mineral Geochem* 55:197–230.
27. Hutcheon ID, Hutchison R (1989) Evidence from the Semarkona ordinary chondrite for Al-26 heating of small planets. *Nature* 337:238–241.
28. Kita NT, Nagahara H, Togashi S, Morishita Y (2000) A short duration of chondrule formation in the solar nebula: Evidence from ^{26}Al in Semarkona ferromagnesian chondrules. *Geochim Cosmochim Acta* 64:3913–3922.
29. Rudraswami NG, Goswami JN, Chattopadhyay B, Sengupta SK, Thapliyal AP (2008) ^{26}Al records in chondrules from unequilibrated ordinary chondrites: II. Duration of chondrule formation and parent body thermal metamorphism. *Earth Planet Sci Lett* 274:93–102.
30. Kunihiro T, Rubin AE, McKeegan KD, Wasson JT (2004) Initial $^{26}Al/^{27}Al$ in carbonaceous chondrite chondrules: Too little ^{26}Al to melt asteroids. *Geochim Cosmochim Acta* 68:2947–2957.
31. Kurahashi E, Kita NT, Nagahara H, Morishita Y (2008) ^{26}Al–^{26}Mg systematics of chondrules in a primitive CO chondrite. *Geochim Cosmochim Acta* 72:3865–3882.
32. Hutcheon ID, Marhas KK, Krot AN, Goswami JN, Jones RH (2009) ^{26}Al in plagioclase-rich chondrules in carbonaceous chondrites: Evidence for an extended duration of chondrule formation. *Geochim Cosmochim Acta* 73:5080–5099.
33. Ushikubo T, Nakashima D, Kimura M, Tenner T, Kita NT (2013) Contemporaneous formation of chondrules in distinct oxygen isotope reservoirs. *Geochim Cosmochim Acta* 109:280–295.
34. Galy A, Young ED, Ash RD, O'Nions RK (2000) The formation of chondrules at high gas pressures in the solar nebula. *Science* 290(5497):1751–1753.
35. Bizzarro M, Baker JA, Haack H (2004) Mg isotope evidence for contemporaneous formation of chondrules and refractory inclusions. *Nature* 431(7006):275–278.
36. Olsen MB, Schiller M, Krot AN, Bizzarro M (2013) Magnesium isotope evidence for single stage formation of CB chondrules by colliding planetesimals. *Astrophys J* 776:L1.
37. Turner NJ, et al. (2014) Transport and accretion in planet-forming disks. *Protostars and Planets VI*, eds Beuther H, Klessen R, Dullemond C, Henning T (Univ Arizona Press, Tucson, AZ), pp 1–24.
38. Nagel E, D'Alessio P, Calvet N, Espaillat C, Trinidad MA (2013) The effect of sublimation temperature dependencies on disk walls around T Tauri stars. *Rev Mex Astron Astrofis* 49:43–52.
39. Faure J, Fromang S, Latter H (2014) Thermodynamics of the dead-zone inner edge in protoplanetary disks. *Astron Astrophys* 564:A22.
40. Desch SJ, Ciesla FJ, Hood LL, Nakamoto T (2005) Heating of chondritic materials in solar nebula shocks. *Chondrites and the protoplanetary disk*, eds Krot AN, Scott ERD, Reipurth B, ASP Conference Series (Astron Soc Pacific, San Francisco), Vol 341, pp 849–872.
41. Charnoz S, Fouchet L, Aléon J, Moreira M (2011) Three-dimensional Lagrangian turbulent diffusion of dust grains in a protoplanetary disk: Method and first applications. *Astrophys J* 737:33–50.
42. Jacquet E, Fromang S, Gounelle M (2011) Radial transport of refractory inclusions and their preservation in the dead zone. *Astron Astrophys* 526:L8.
43. Lesur G, Kunz MW, Fromang S (2014) Thanatology in protoplanetary discs: The combined influence of Ohmic, Hall, and ambipolar diffusion on dead zones. *Astron Astrophys* 566:A56.
44. Meheut H, Meliani Z, Varniere P, Benz W (2012) Dust-trapping Rossby vortices in protoplanetary disks. *Astron Astrophys* 545:A134.
45. Kruijer TS, et al. (2014) Protracted core formation and rapid accretion of protoplanets. *Science* 344(6188):1150–1154.
46. Ingalls SC, Young ED, Gounelle M (2012) Do magnesium isotope systematics of Al-rich chondrules offer insights into the history of chondrule formation in general? *43rd Lunar Planet Sci Conf* 43:2665.
47. Lodders K (2003) Solar system abundances and condensation temperatures of the elements. *Astrophys J* 591:1220–1247.